Hueckel, T., François, B. & Laloui, L. (2009). *Géotechnique* **59**, No. 3, 197–212 [**doi:** 10.1680/geot.2009.59.3.197]

Explaining thermal failure in saturated clays

T. HUECKEL*, B. FRANÇOIS† and L. LALOUI†

Failure conditions in soils at elevated temperatures appear to be strongly dependent on the history of the application of stress and temperature. Four cases of such history leading to various modes of failure are identified and interpreted in terms of thermal Cam-clay models. Particular attention is given to the influence of thermal variability on the coefficient of the critical state, *M*, or the angle of internal friction. A detailed analysis of the material history offers an explanation of an apparent confusion about whether the soil strength is decreased or increased by temperature. In a companion paper, numerical analysis of the development of axisymmetric thermal and stress fields around a cylindrical heat source suggests that thermal failure may arise in conditions that are far from any mechanically critical situation.

KEYWORDS: failure; triaxial test; temperature effects; clays

Les conditions de rupture dans les sols soumis à des températures élevées sont fortement dépendantes de l'histoire des contraintes et des températures appliquées. Quatre cas de telles histoires de chargement menant à différents modes de ruptures sont identifiés et interprétés dans le contexte d'un Cam-Clay non-isotherme. Une attention particulière est accordée à l'influence de la variation avec la température du coefficient de l'état critique, M, ou de l'angle de frottement interne. Une analyse détaillée de l'histoire du matériau offre une explication à une confusion existante quant à la diminution ou l'augmentation de la résistance au cisaillement des sols chauffés. Dans un article complémentaire, des simulations numériques de développement de champs thermiques et de contraintes en conditions axisymétriques autour d'une source de chaleur sont présentés. Elles suggèrent que la rupture thermique peut se produire dans des conditions qui sont fort éloignées de toute instabilité mécanique.

INTRODUCTION

Thermal failure is broadly understood as a class of diverse failure conditions in soils, generated by or in the presence of elevated temperature. Any analysis of failure mechanisms pertinent to any underground structure subject to heat needs to be extended to include the response of soil to heating, and the effect of temperature on soil mechanical properties. Geotechnical structures exposed to heat may suffer alterations of their original, or isothermal, macroscopic mechanical properties owing to a series of physical phenomena at the microstructural level, such as differences in the thermal expansion of solids and water, mineral debonding, or alterations of adsorption forces in clay water (Baldi *et al.*, 1988). Several such alterations have been documented in laboratory experiments, and are believed to be crucial in the design of underground structures that are subject to thermal variations. Such structures are often part of emerging technologies, including energy storage in soil using geostructures such as piles, walls and slabs for environmentally friendly heating and cooling of buildings (Brandl, 2006; Laloui *et al.*, 2006). Another emerging technology involving thermally affected soil masses is oil recovery from reservoirs that are at high pressure and high temperature (Hahn *et al.*, 2003). Finally, in the design of underground nuclear waste disposal facilities, which have been in development for several decades, the effects of temperature are invariably considered as a principal factor (e.g. Gens & Olivella, 2001; Laloui *et al.*, 2008). Notably, such structures are often prototypes, the long-term performance of which demands intense monitoring. Monitoring system design requires prior numerical simulations and clearly a capability to model soil behaviour under non-isothermal conditions.

Manuscript received 18 June 2008; revised manuscript accepted 7 November 2008.
Discussion on this paper closes on 1 September 2009, for further details see p. ii.
* Duke University, Durham, NC, USA.
† Ecole Polytechnique Fédérale de Lausanne, EPFL, Switzerland.

While substantial progress has been made in understanding the principal effects of elevated temperature in soil mechanics, the failure conditions remain less well understood. In fact, there is a somewhat confusing view of the experimental evidence concerning the thermal dependence of shear strength (Mitchell, 1964; Bourros, 1973; Borsetto *et al.*, 1984; Houston *et al.*, 1985; Hueckel & Baldi, 1990; Kuntiwattanakul *et al.*, 1995; Jefferson *et al.*, 1996; Burghignoli *et al.*, 2000; Cekerevac & Laloui, 2004). The confusion seems to arise from insufficient emphasis having been placed on the thermal and mechanical history of the material prior to failure.

The peculiarities of the mechanical response of soil to heating established in early experiments consist in a substantial thermoplastic contraction in normally and slightly overconsolidated soils, as opposed to the thermoelastic expansion of heavily overconsolidated soils, as well as a possibility of thermal failure during undrained heating at a constant non-isotropic stress (Campanella & Mitchell, 1968; Plum & Esrig, 1969; Borsetto *et al.*, 1984; Baldi *et al.*, 1988; Hueckel & Baldi, 1990; Hueckel & Pellegrini, 1992). These experimental results initially led to the idea of extending Prager's (1958) metal thermoplasticity to soils. This produced a thermal Cam-clay model (Borsetto *et al.*, 1984; Hueckel *et al.*, 1987; Hueckel & Pellegrini, 1989; Hueckel & Borsetto, 1990). Since these initial developments, a substantial amount of additional experimental evidence and new modelling ideas have been added (Laloui, 1993; Picard, 1994; Tanaka *et al.*, 1997; Cui *et al.*, 2000; Laloui & Cekerevac, 2003, 2008; François & Laloui, 2008), which have thrown new light on the initial concepts.

In this paper we examine some of the elements of the thermal history of clay, and its role in reaching failure. An extension of thermal conditions to the Cam-clay family of models is used to explain the differences. New aspects of the re-evaluated thermal sensitivity of the critical state coefficient (or internal friction angle) (for more details see Hueckel & Laloui, 2009) are discussed.

THERMOMECHANICS OF SOILS

Thermal sensitivity of the apparent preconsolidation stress

The key thermal effects in soils, at least in some applications, are those that lead to irreversible changes, particularly irreversible deformation. To address the irreversible strain in thermal conditions, the classical notion of the elasticity domain in the elasto-plastic context must be revised. The main new feature is the strong sensitivity of the plastic limit to temperature. This finding is expected, as most materials exhibit such sensitivity. However, other prominent thermomechanical characteristics of soils that need to be considered in this context are clearly different from those of other materials (e.g. metals), and are summarised as follows, based on the experimental work cited above.

(*a*) At zero external stress or high overconsolidation ratio (OCR), thermal strain under constant-stress drained heating conditions is expansive and reversible, and is often dependent on the effective stress.
(*b*) At high external effective stress or low OCR (close to normally consolidated conditions), thermal strain under constant-stress drained heating conditions is compressive and irreversible.
(*c*) Preconsolidation isotropic stress in an unstressed soil is temperature dependent: the higher the temperature, the lower the 'apparent preconsolidation pressure'.
(*d*) A thermal cycle of drained heating and cooling for low effective stress (high OCR) is reversible as far as the apparent preconsolidation pressure is concerned, but for higher stress (low OCR), when irreversible strain is generated during heating, the post-cycle apparent preconsolidation pressure may be significantly higher than the original pressure.
(*e*) The plastic strain rate during heating at constant (near K_0) stress in some tests deviates greatly from the normality rule towards isotropic states (scarce and limited data).
(*f*) In undrained conditions, under normally consolidated conditions, large pore pressure can be generated during heating, again depending on the effective stress.

On the basis of these observations, the elasticity domain is thought of as temperature dependent, shrinking when soil is heated and expanding during cooling (Fig. 1). As in a single yield surface plasticity, the soil behaviour upon shearing depends on the current apparent preconsolidation stress: thermal changes of the latter will affect the evolution of the former. Hence a specific form of the temperature dependence of the apparent preconsolidation stress has a critical impact on the thermal failure. An additional important factor appears to be the thermal evolution of the critical stress state locus (variable M).

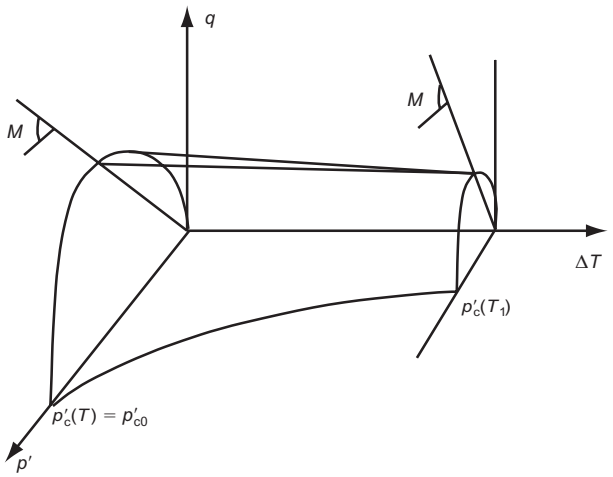

Fig. 1. Evolution of yield locus with temperature increase (at no heat-induced plastic strain): q, principal stress difference; p', mean effective stress; T, temperature (adapted from Hueckel, 1992)

In the thermal Cam-clay model (Hueckel & Borsetto, 1990), the elastic domain is represented through a relationship between the isotropic mean effective stress and the deviatoric stress invariant (p' and q respectively), as well as the temperature T. The yield locus is considered either as an ellipse (modified Cam-clay locus; Roscoe & Burland, 1968), equation (1), or a logarithmic function (original Cam-clay locus; Schofield & Wroth, 1968), equation (2). It is assumed that the reader is familiar with the concepts of the isothermal Cam-clay model (see e.g. Muir Wood, 2004, for a concise presentation).

$$f = p'^2 - p'\,p'_{\mathrm{c}} + \left(\frac{q}{M}\right)^2 = 0 \tag{1}$$

$$f = \frac{q}{Mp'} + \ln\left(\frac{2{\cdot}718\,p'}{p'_{\mathrm{c}}}\right) - 1 = 0 \tag{2}$$

The apparent preconsolidation stress p'_{c} denotes the size of the locus along the isotropic effective stress axis, p'. Its temperature dependence is believed to be valid during both heating and cooling: hence it is postulated to be a one-to-one relationship. Note that, rather than the absolute temperature, we consider its difference $\Delta T = T - T_0$ relative to a reference temperature value T_0, at which all parameters, particularly $p'(\Delta T = 0) = p'_{\mathrm{c}0}$, are measured. Hueckel & Borsetto (1990) assumed the following format for p'_{c}:

$$p'_{\mathrm{c}} = p'_{\mathrm{c}0}\exp\left[\frac{1}{\lambda-\kappa}(1-a_0\Delta T)(1+e_0)\varepsilon_{\mathrm{v}}^{\mathrm{p}}\right] + 2\left(a_1\Delta T + a_2\Delta T^2\right) \tag{3}$$

The last term on the right-hand side of equation (3) represents the thermal softening function, and λ and κ are the isotropic moduli of the elasto-plastic and elastic incremental compressibilities of soil respectively; e_0 is the initial value of the void ratio. The coefficients a_i ($i = 0$, 1, and 2) are constant. Equation (3) actually represents the thermoplastic hardening/softening rule. As a result, the plastic compressibility modulus is temperature dependent.

Since the original formulation of the thermal softening function (equation (3)), several alternative representations have been proposed (e.g. Picard, 1994; Gera *et al.*, 1996). In this paper we also use an alternative thermal softening function (Laloui & Cekerevac, 2003), which acts as an amplifier of the plastic strain-hardening effect:

$$p'_{\mathrm{c}} = p'_{\mathrm{c}0}\exp\left(\frac{1+e_0}{\lambda-\kappa}\varepsilon_{\mathrm{v}}^{\mathrm{p}}\right)\left[1-\gamma\log\left(1+\frac{\Delta T}{T_0}\right)\right] \tag{4}$$

where γ is a material parameter.

As a result, the plastic strain-hardening and thermal softening play a multiplicative role on each other. Because of this, the bulk modulus in this formulation is temperature independent.

In the following, both formulations will be used. We consider them as alternatives that have the same set of underlying principles.

Thermal sensitivity of the critical state

The apparent preconsolidation pressure is not the only yield locus characteristic that may evolve with temperature. The confusing experimental evidence on the thermal dependence of shear strength points to the possibility of an actual

change of the critical state with temperature. This assumption has been discussed before (Hueckel, 1992, 1997; Laloui, 1993), based on experimental data on Boom clay, for which a variation of $M(\Delta T)$ was observed, as opposed to Pontida clay, which is seemingly insensitive to temperature (Hueckel & Pellegrini, 1991). In addition, systematic investigations on kaolinite have pointed to a very clear growth of M (Cekerevac & Laloui, 2004).

It is fair to say that the intensity of the dependence of the critical state line in the q–p' plane, represented by the slope M, is most likely material specific. A clear problem is that a very limited change in the value of the coefficient of critical state M (20%/$\Delta T = 70$°C increase for the Boom clay, and at most 12·5%/$\Delta T = 68$°C for kaolin CH1) may bring about a significant change in the shear strength. Despite such early observations, little has been done to include it into the constitutive modelling, or to use it in the interpretation of experimental results.

The fact that there are two different sources of sensitivity of the yield locus to temperature affects the form of the flow rule. In particular, if (Hueckel & Laloui, 2009)

$$p'_c = p'_c\left(\varepsilon_v^p, \Delta T\right); \qquad M = M(\Delta T) \tag{5}$$

then Prager's consistency condition requires that, to maintain the yielding process,

$$\mathrm{d}f = \frac{\partial f}{\partial \boldsymbol{\sigma}'} : \mathrm{d}\boldsymbol{\sigma}' + \frac{\partial f}{\partial p'_c}\mathrm{d}p'_c + \frac{\partial f}{\partial M}\frac{\partial M}{\partial T}\mathrm{d}T = 0 \tag{6}$$

Hence, if the flow rule is assumed to be associated, that is if

$$\mathrm{d}\varepsilon_v^p = d\lambda \frac{\partial f}{\partial p'}; \quad p' = tr\boldsymbol{\sigma}' \tag{7}$$

as $\mathrm{d}p'_c = \mathrm{d}p'_c(\mathrm{d}\varepsilon_v^p, \mathrm{d}T)$, the plastic multiplier $\mathrm{d}\lambda$, which controls the amount of the plastic strain rate, is affected by the change in M:

$$\mathrm{d}\lambda = \frac{1}{H}\left[\frac{\partial f}{\partial \boldsymbol{\sigma}'} : \mathrm{d}\boldsymbol{\sigma}' + \left(\frac{\partial f}{\partial p'_c}\frac{\partial p'_c}{\partial T} + \frac{\partial f}{\partial M}\frac{\partial M}{\partial T}\right)\mathrm{d}T\right] \geqslant 0;$$

$$H = -\frac{\partial f}{\partial p'_c}\frac{\partial p'_c}{\partial \varepsilon_v^p}\frac{\partial f}{\partial p'} \tag{8}$$

Therefore the plastic strain increment is affected by the thermal variation of internal friction (i.e. M), as long as $q \neq 0$. Otherwise, this dependence disappears, as for both forms of the yield locus (equations (1) and (2)) $\partial f/\partial M = 0$ if $q = 0$. In addition, $\mathrm{d}p'_c = 0$.

At any constant effective stress during heating along with continuing plastic yielding, there is a specific plastic strain increment generated per increment of temperature,

$$\frac{\mathrm{d}\varepsilon_v^p}{\mathrm{d}T} = \frac{1}{H}\frac{\partial f}{\partial p'}\left(\frac{\partial f}{\partial p'_c}\frac{\partial p'_c}{\partial T} + \frac{\partial f}{\partial M}\frac{\partial M}{\partial T}\right) \tag{9}$$

Equation (9) describes a compensatory thermoplastic hardening mode in which plastic strain-hardening compensates for thermal softening. In addition, in the case of heating at a constant effective stress ($q \neq 0$), the consistency condition (equation (6)) restrains the evolution of p'_c and M during the temperature change:

$$\mathrm{d}p'_c = -\left(\frac{\partial f}{\partial M} \Big/ \frac{\partial f}{\partial p'_c}\right)\mathrm{d}M \tag{10}$$

In other words, changes in M need to be compensated for by necessary adjustments in terms of changes in p'_c. Fig. 2

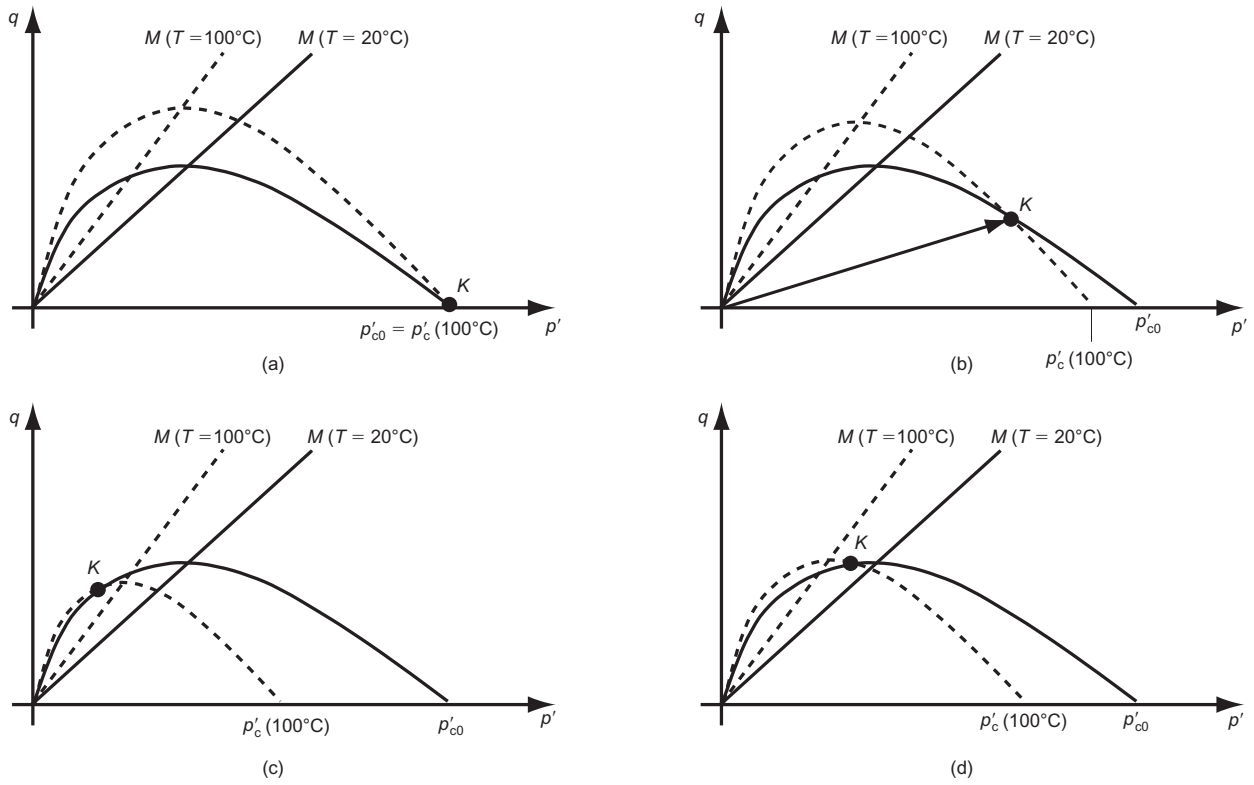

Fig. 2. Examples of evolution of (original) Cam-clay yield locus during heating from 20°C to 100°C at constant stress state, stress point K, at continuous yielding: (a) when stress state is purely isotropic; (b) when stress state has a non-zero deviatoric component, $q \neq 0$, and $p' > p'_{c0}/2{\cdot}718$; (c) when stress state has a non-zero deviatoric component and $p' < p'_c/2{\cdot}718 < p'_{c0}/2{\cdot}718$; (d) when stress state has a non-zero deviatoric component and $p'_c/2{\cdot}718 < p' < p'_{c0}/2{\cdot}718$

shows four particular cases of the original Cam-clay yield locus evolution, affected to maintain a constant effective stress state K at yielding. It must be emphasised that this type of loading is very important, as it includes heating at a K_0 state, which is a common in situ stress state.

THERMAL FAILURE: STRESS AND THERMAL HISTORY DEPENDENCE

The most important factor in understanding the temperature dependence of the failure condition appears to be the preceding thermal and mechanical soil history. Four cases of different stress histories will be discussed below:

(*a*) isotropic drained heating at a high OCR followed by drained triaxial compression
(*b*) isotropic drained heating at normal consolidation or an intermediate to low OCR, followed by drained triaxial compression
(*c*) isotropic drained or undrained heating, followed by undrained triaxial compression
(*d*) undrained heating at a non-isotropic constant total stress.

Drained triaxial thermal failure after drained heating of high-OCR clays: temperature effect

The most important distinction of this type of thermo-mechanical loading history is that no thermoplastic strain is produced during heating. In other words, it is ensured that the stress never satisfies the yielding condition (which evolves with temperature). This implies that the yield locus evolution depends only on temperature. The earliest tests of this kind were conducted on remoulded Pontida silty clay (for test details and material characterisation see Hueckel & Baldi, 1990; Baldi *et al.*, 1991) and high-carbonate Spanish clays SS-1 and IC-1 (Del Olmo *et al.*, 1996; Hueckel *et al.*, 1998).

Pontida clay. Pontida clay was tested at 23°C and 95°C or 98°C, and at two values of confining effective stress, 0·2 MPa (OCR = 12·5) and 0·5 MPa (OCR = 5; $p'_{c0} = 2{\cdot}5$ MPa). The results are shown in Figs 3(a) and 3(b).

From the isotropic heating data for Pontida clay (Hueckel & Baldi, 1990), it can be calculated that the apparent preconsolidation stress during heating decreases from 2·5 MPa to about 1·52 MPa. Consequently, the triaxial trajectories of the confining stress at 0·2 MPa and 0·5 MPa are in the elastic domain from the onset of triaxial loading until they intersect the yield locus. The yielding upon shearing at elevated temperature is met below the analogous stress values reached at ambient temperature (Fig. 3). Indeed, the experimental curves at 98°C have lower peak stresses than that at 22°C. Clearly, the critical state is reached at the same stress at both temperatures.

It appears that high temperature produces a more ductile behaviour (less softening) than low temperatures. Such ductilisation is consistent with the behaviour of many other solids, such as steel (Argon, 2001) and granite (Wong, 1982). Softening, which is seen at room temperature at 0·2 MPa, disappears at 98°C. In terms of deformation, the notable dilatancy seen during triaxial compression at room temperature at 0·2 MPa transitions at 98°C to a constant-volume shear at larger strain. At 0·5 MPa the room temperature dilatancy also disappears, in favour of an initial compaction followed by a constant-volume shear. Clearly, the soil state is closer to the normally consolidated state at elevated temperature than at ambient temperature, for the same confining pressure, as discussed at length by Hueckel & Baldi (1990).

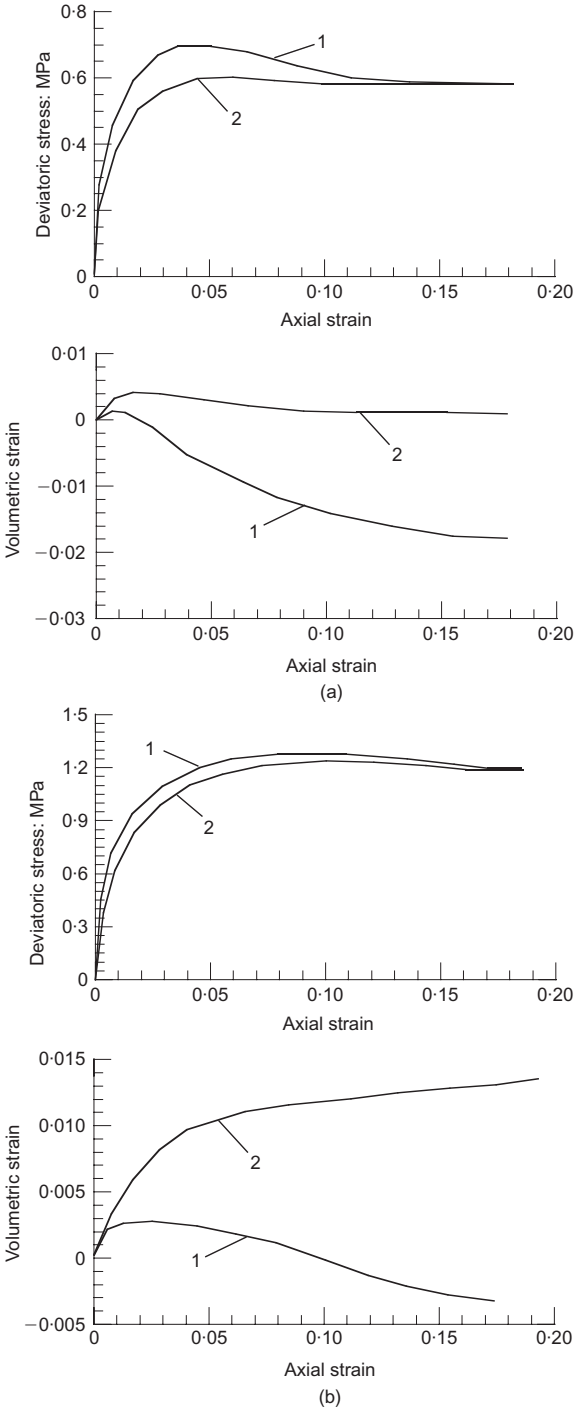

Fig. 3. Deviatoric stress against axial strain and volumetric strain during triaxial loading of Pontida silty clay at (1) 22°C and (2) 98°C, at confining effective stress of: (a) 0·2 MPa, equivalent to OCR = 12·5; (b) 0·5 MPa, equivalent to OCR = 5 (after Hueckel & Baldi, 1990)

High-carbonate Spanish clay. The evolution of a single peak stress in triaxial compression with temperature at a relatively low confining stress of 0·75 MPa (OCR = 6) with a sequence of increasing temperature values was investigated in test SS-18 on a carbonate clay (initial void ratio of 0·51) from series SS-1 from Spain (Hueckel *et al.*, 1998). Because of a significant heterogeneity of the specimen population, the test was conducted on a single specimen using the multiple loading technique in triaxial compression (Drescher *et al.*, 1974; see also Kovari & Tisa, 1975). This technique is adapted as follows (Fig. 4(a)). The soil was first compressed triaxially at 22°C and 0·75 MPa up to the peak stress value,

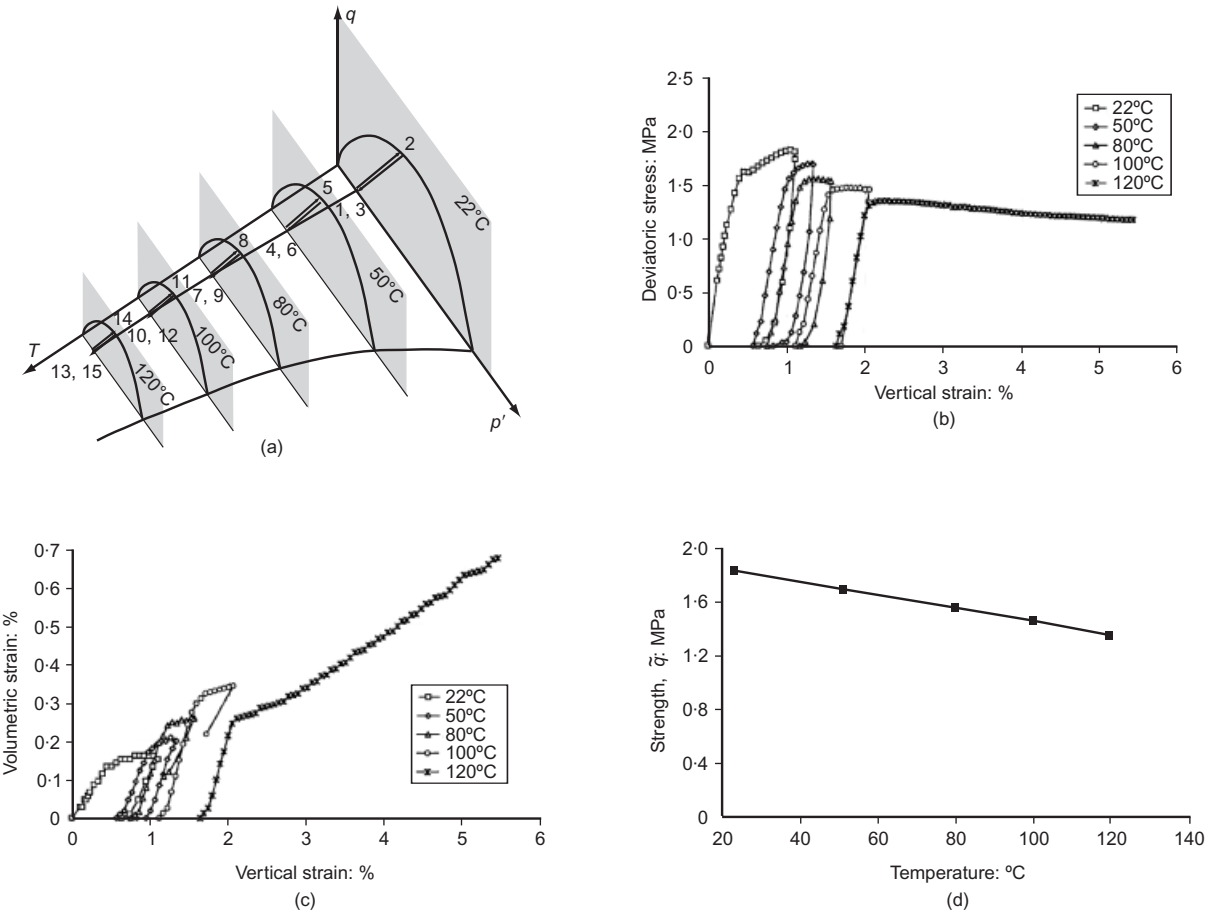

Fig. 4. Multiple loading technique performed on a sample of Spanish clay, triaxial test SS-18 at 0·75 MPa confining stress heated to different temperatures: (a) thermomechanical triaxial loading trajectory in the thermoelastic domain; (b) stress–strain curve; (c) volumetric strain; (d) shear strength

but not beyond, and unloaded back to $q = 0$. Next, the same specimen was heated to 50°C at isotropic stress (0·75 MPa) in drained conditions. At this temperature, subsequent drained triaxial compression was started, but interrupted again at the peak stress. The interruption at the peak prevents the development of any strain-softening, as understood in Cam-clay theory, and thus any observed strength drop, compared with 22°C, is attributed to thermal softening alone. Subsequently, cycles of unloading, further increase in temperature, and triaxial compression were performed at 80°C, 100°C and 120°C. Interruption of the triaxial loading was actuated when three consecutive stress increment readings were below a previous maximum.

The observed peak deviatoric stress decreases with temperature in the range $20°C < T < 120°C$ (Fig. 4(b)), and shows a nearly linear dependence on temperature (Fig. 4(d)). No (or very limited) plastic strain is produced during heating, as there is no contact between the stress point and the yield locus. Hence the strength decrease is dependent only on temperature. Indeed, no plastic (compressive) vertical strain difference is seen between the completion of each triaxial unloading and the onset of the subsequent triaxial reloading (Fig. 4(c)), while the volumetric strain differences are all expansive. The overall reduction of strength over the span of 100°C amounts to about 25% of the reference room-temperature strength value. This is not a substantial effect compared with possible thermal strength reductions of up to 90% occurring in some rocks (Wong, 1982; Hueckel *et al.*, 1993).

Notably, the triaxial strength at a constant effective confining stress and the maximum apparent isotropic preconsolidation stress at any given temperature are not independent if a one-to-one relationship is postulated to exist, as represented by the equations of the yield condition in the Cam-clay models (equations (1) or (2); see also schematic in Fig. 4(a)). Thus, assuming the yield locus of the original Cam-clay, the effect of temperature on the preconsolidation pressure can be deduced from the evolution of the peak deviatoric stress $\tilde{q}$ with T.

It is clear that the thermal changes in triaxial strength are far more modest than those that could be extrapolated from the isotropic heating tests. The experimental value of peak deviatoric stress at a temperature of 22°C, considered as a reference temperature, at the confining stress of 0·75 MPa is 1·85 MPa. Considering a constant $M = 1·04$ (as determined from the residual state of Fig. 4(b)), this deviatoric strength corresponds to the apparent preconsolidation effective stress of $p'_{c0} = 5·02$ MPa (Fig. 5). This value is relatively close to the preconsolidation pressure of 4·5 MPa that was independently determined by Hueckel *et al.* (1998). At 120°C, the peak deviatoric stress is 1·37 MPa and the corresponding $p'_c = 3·59$ MPa. This thermal softening effect seems lower than that predicted through the measurement of the volumetric thermoplastic strain in isotropic heating tests (Del Olmo *et al.*, 1996; Hueckel *et al.*, 1998). This result may indicate that the coefficient M is not actually constant in this material. We address this question below. Interestingly, although no plastic strain was intentionally produced in this test, those incipient volumetric strain rates that did occur indicate an evolution from a dilatant behaviour at 22°C and 50°C to compactant behaviour at 80°C and 100°C, and completely compactant behaviour at the terminal phase at 120°C.

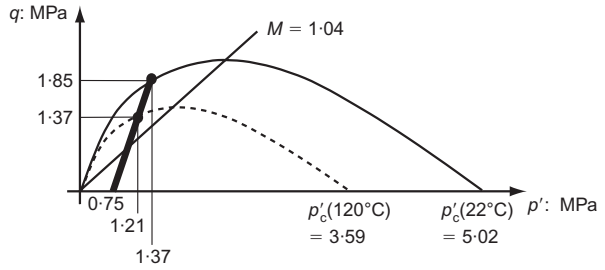

Fig. 5. Comparison between stress paths followed by the carbonate-rich Spanish clay during triaxial compression at 22°C and 120°C with the deduced original Cam-clay yield limit (M = const.)

One of the possible explanations for the disparity between the thermal sensitivity of the apparent preconsolidation stress and that of the triaxial strength is that they are actually independent functions of ΔT, which translates into the hypothesis that the coefficient M, and hence the internal friction angle, are both dependent on ΔT.

The results in Fig. 4(d) present a good opportunity to discuss this possibility. Hueckel *et al.* (1998) discussed at length the evolution of the peak strength with temperature, and concluded that under constant M there is a lower bound to the decrease of strength, which occurs at a critical temperature corresponding to the triaxial strength at the intersection of the given stress path and the critical line. Above that critical temperature, the strength remains at the critical value.

This is not the case when $M = M(\Delta T)$. As the shape and characteristic dimensions of the yield locus are controlled by two independent functions of ΔT, the outcome may be quite different, as shown in Figs 6(a) and 6(b), and Fig. 2. First, the peak strength on a given stress path may vary non-monotonically, first decreasing and then increasing, and remain above the critical line. Second, if the peak strength does decrease monotonically, then at some temperature T_{crit} it reaches a value at a current critical line (70°C in the example in Fig. 6(a)), at $\tilde{q}_{crit}$. However, as temperature increases and the yield locus continues to shrink, say to 90°C, the yield point changes from the strain-softening side to the strain-hardening part of the locus. Hence subsequent triaxial loading at that temperature produces yielding at f_{90}, but strain-hardening allows the locus to grow until it reaches the current critical line at M_{90}, and hence possibly at a much higher $\tilde{q} > q_{crit}$. For M = const. = M_{22} for $T > T_{crit}$, all possible hardening curves end up at $\tilde{q} = q_{crit}$ (see Hueckel *et al.*, 1998). This may be an explanation for the observation of Rousset *et al.* (1992) of a minimum $\tilde{q}$ at around 80°C for Aisne clay. While no such minimum was detected for SS-1 clay for $T < 120$°C, no data are available on the actual variability of M for this clay.

Similar behaviour, with the overconsolidated strength decreasing with temperature and concomitant ductilisation, has been reported for Boom clay (Baldi *et al.*, 1991, 1993). Tanaka *et al.* (1997) also reported on decreasing yield and peak stresses with temperature up to 100°C for Canadian illitic clay at intermediate and low OCRs. However, stress–strain curves are not available for an individual evaluation. In a series of triaxial compression tests following drained heating or cooling to up to 50°C, Marques *et al.* (2004) also reported a drop in peak strength with temperature in a sensitive surficial Canadian clay.

Drained triaxial thermal failure after drained heating of low-OCR (or NC) clays: combined temperature and thermoplastic strain effects

The principal characteristic of drained heating at constant stress of normally consolidated soil or soil at intermediate OCR (prior to the triaxial loading) is the thermoplastic strain generated over at least a portion of the heating process. The yielding arises when the shrinking yield locus reaches the imposed constant stress value. In the subsequent process, the resulting thermoplastic strain-hardening compensates for the thermal softening to maintain p'_c = const. Fig. 7 shows that the heating process may induce a normally consolidated state of the material at elevated temperature that was originally at an intermediate OCR at room temperature. The subsequent triaxial compression produces normally consolidated behaviour at elevated temperature, as opposed to the overconsolidated response that develops at room temperature. This type of loading is a close representation of many in situ circumstances.

Tests of this kind on kaolin clay (remoulded) were reported by Cekerevac & Laloui (2004). Heating was conducted at room temperature and at 90 °C. Fig. 8 shows the results for an NC sample at OCR = 1·5, 2 and 3.

Three main trends are visible in those results. First, similar to the Pontida silty clay (Fig. 3), the maximum deviatoric stresses reached in triaxial compression at 90°C and 22°C differ, but not significantly. However, the difference is consistently opposite to that seen in Pontida, Boom, and Spanish clays: the stress values at 90°C are generally

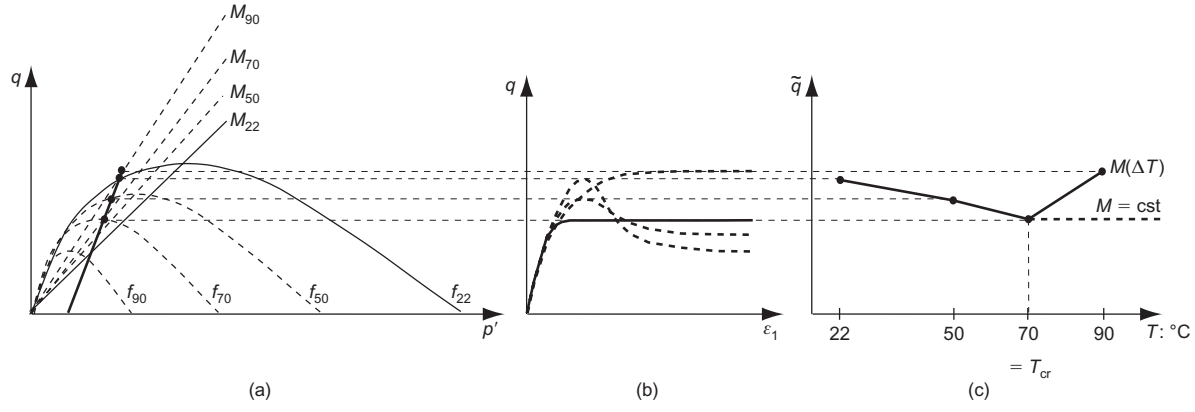

Fig. 6. Evolution of peak strength $\tilde{q}$ at constant lateral stress with temperature: (a) for peaks at the softening part, $\tilde{q} > \tilde{q}_{crit}$, the strength can decrease with temperature, whereas for the yield locus it shrinks below $\tilde{q} < \tilde{q}_{crit}$, and the ultimate strength is reached through a hardening process always at the value of the stress path intersection with the current critical state line $M(\Delta T)$; (b) corresponding stress–strain curves; (c) theoretical variation of strength with temperature. Note that for M = const., strength remains constant at $\tilde{q}_{crit}$ (Hueckel *et al.*, 1998)

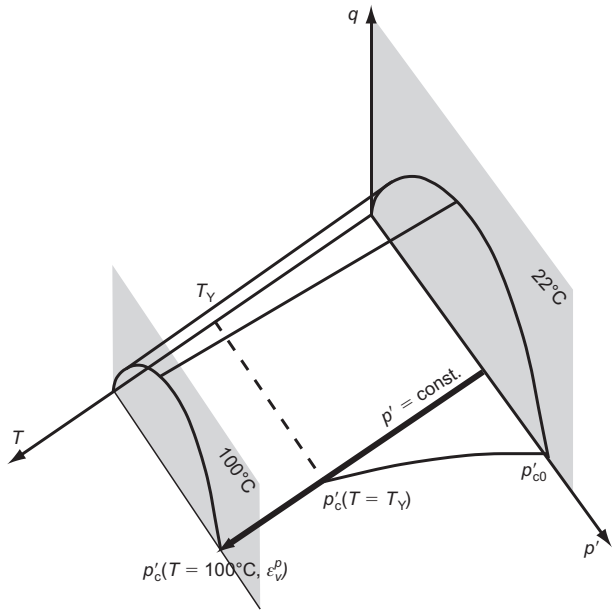

Fig. 7. Changes in yield locus major axis, p'_c, at constant effective stress in conjunction with thermally induced changes in the apparent preconsolidation stress p'_c and a compensating thermoplastic strain-hardening (not shown) starting at T_Y

greater than those at 22°C, including the peak values. Notably, a manifestation of loss of stability is seen in both the cold and the hot tests at an advanced strain, as a second-order work non-positiveness (Bigoni & Hueckel, 1991; Muir Wood, 2004). Second, the initial part in the hot test is more rigid than in the cold specimens. Third, in terms of the volumetric strain, the hot samples are less contractile than the cold samples at all low-OCR tests. This is again opposite from what is seen in Pontida and Boom clays. This set of seemingly contradictory findings may be explained using a systematic analysis of the hardening response within its representation in the p', T and ε_v space. This is shown in Fig. 9, which shows a schematic of p'_c as a function of both ΔT and ε_v^p for $M = \text{const.}$. A more general case with $M(\Delta T)$ is discussed below.

From the point of view of the thermal history of the yield locus, the tests of Cekerevac & Laloui (2004) on kaolin clay with heating at isotropic stress states fell into two categories, depending on the OCR. In this section, the NC and low-OCR tests are of interest.

In normally consolidated specimens, heating starts and continues through when the material yields, generating significant contractile volumetric plastic strain by way of the compensatory hardening mechanism to counter the effect of thermal softening. In the stress space projection (Fig. 9, bottom graph), the constant-stress condition is visualised as point B at an immobile projection of the yield locus. In the hardening space (top graph), it is represented by way of a T, ε_v^p path in a $p'_c = \text{const.}$ plane, starting from point B′ and showing a corresponding amount of the plastic compaction strain at point C′. Consequently, when the material is subsequently subjected to triaxial compression at constant temperature from point C to failure, F, it requires less additional volumetric plastic strain, represented by C′F′, to reach the final yield surface position p'_{cf} than in an analogous process for a cold specimen between p'_{c0} and p'_{cf}, represented here by segment B′D.

In reality, the amount of volumetric strain generated by heating is not very large relative to the triaxial compression volumetric strain: 0·8% compared with 6%. As a result, the difference in terms of the volumetric strains during triaxial compression is relatively small between hot and cold specimens, but it conforms to the tendency of the model. In addition, the stiffness, which during triaxial compression may be represented by the ratio between the axial stress and axial strain, is larger in the post-heating phase: that is, hot samples are stiffer than cold samples.

For low values of OCR (1·2, 1·5, 2 and 3), less thermoplastic strain (than in the NC case) is produced during the heating phase. The first part of the response to heating is thermoelastic (Cekerevac & Laloui, 2004), and involves free shrinking of the yield locus affected by temperature change only, which is halted at the imposed value of stress. During further heating, the compensation mechanism is activated as in the NC case above. The triaxial loading follows the same stress path, in the q–p' plane, at high and low temperature. Indeed, the maximum axial stress is the same, and is defined by the same critical line. However, at 22°C the triaxial loading starts elastically at an overconsolidated state, crossing a yielding point at a certain stress level. By contrast, at 90°C the triaxial path generates elasto-plastic strain from the very beginning, but is stiffer, owing to the previous accumulation of thermoplastic strain during heating. As a result, the contractile volumetric strain produced is lower.

For all stress paths for kaolin CH1 it appears that the peak stress is consistently about 10% higher in the hot samples than in cold ones (Fig. 9). The corresponding stress paths clearly cross over the isothermal critical line. A marked post-peak softening is seen as a manifestation of material behaviour instability and localisation (e.g. Bigoni & Hueckel, 1991): hence it is beyond the framework of incremental constitutive laws, and is not considered.

In addition, materials such as the Boom and Spanish clays exhibit much lower thermal reductions in triaxial strength at mid to high OCRs than that predicted based on the assumption that $M = \text{const.}$ (Baldi *et al.*, 1991, 1993).

Hence it is proposed that the thermally induced variation in the critical state—that is, in internal friction angle—is a factor in the evolution of peak thermal strength. In reference to Fig. 2(a), one can anticipate that during isotropic heating of an M-temperature-sensitive material, the evolution of the yield locus is composed of two portions:

(*a*) for $p' < p'_c$, in an elastic state of stress, the thermal shrinking of p'_c with temperature, concomitant with a thermally induced increase in $M(\Delta T)$, and in the minor semi-axis of the yield locus $q^* = M(\Delta T)p'_c(\Delta T)/\beta$, where $\beta = 2$ in modified Cam-clay (equation (1)) and $\beta = 2{\cdot}718$ in original Cam-clay (equation (2))

(*b*) at constant $p' = p'(\Delta T, \varepsilon_v^p)$, with a compensatory mode thermoplastic strain-hardening, concomitant with an independent thermally induced increase in $M(\Delta T)$.

As for the resulting evolution of the yield locus, this comprises a shrinking of the first portion due to the thermal decrease in p'_c with the superposed growth in q^*. For an arbitrary but constant p', the corresponding stress difference change $\mathrm{d}q$ at yielding for the modified Cam-clay locus ($\beta = 2$), equation (1), can be derived from equation (6) as

$$\mathrm{d}q = \left(p' \frac{\partial p'_c}{\partial T} + \frac{2q^2}{M^3} \frac{\partial M}{\partial T} \right) \frac{M^2}{2q} \mathrm{d}T \tag{11}$$

Noting that $\partial p'_c/\partial T < 0$, whereas $\partial M/\partial T > 0$, the resulting $\mathrm{d}q$ may be either positive or negative for $\mathrm{d}T > 0$, and hence the peak strength may increase or decrease for increasing temperature.

In the second portion of the process, the apparent preconsolidation pressure remains constant, $p'_c = p'_c(\Delta T, \varepsilon_v^p) = \text{const.}$, so that $(\partial p'_c/\partial \varepsilon_v^p)\mathrm{d}\varepsilon_v^p + (\partial p'_c/\partial T)\mathrm{d}T = 0$, concomitant with an independent thermally induced continuing increase in

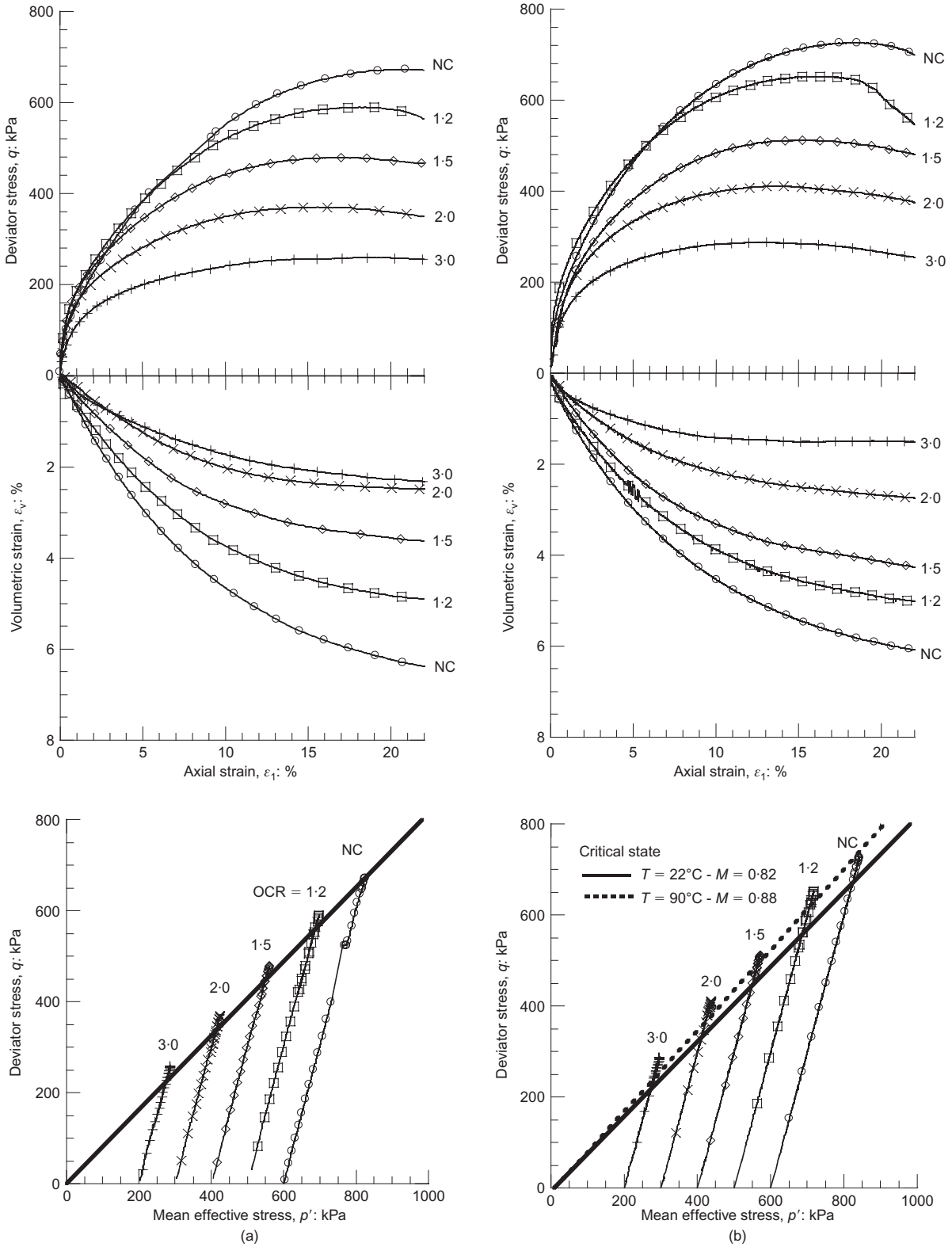

Fig. 8. Results of triaxial compression tests at 22°C and 90°C on kaolin CH1 (Cekerevac & Laloui, 2004): representations in the q–ε_1, ε_v–ε_1 and q–p' planes

$M(\Delta T)$, and a reduction in the minor semi-axis of the yield locus. The amount of ε_v^p generated in this process depends on $(\partial p_c'/\partial T)\mathrm{d}T$ and $\partial p_c'/\partial \varepsilon_v^p$, but is independent of $\partial M/\partial T$. For an arbitrary but fixed p', the corresponding stress difference change at yielding for the Modified Cam-clay locus (equation (1)) is always positive, given by

$$\mathrm{d}q = \left(\frac{2q^2}{M^3}\frac{\partial M}{\partial T}\right)\frac{M^2}{2q}\mathrm{d}T > 0 \tag{12}$$

as $\partial M/\partial T > 0$ and $\mathrm{d}p_c' = 0$ in this portion of the process: hence 'the shrinking' in the deviator, q, is not possible.

As a result, for an arbitrary OCR, the accumulated change in q at $p' = \text{const.}$, given by

$$\Delta q = \int_{T_0}^{T_y} \mathrm{d}q(\mathrm{d}T) + \int_{T_y}^{T_f} \mathrm{d}q(\mathrm{d}T) \tag{13}$$

can be either positive or negative, but is a predictable result

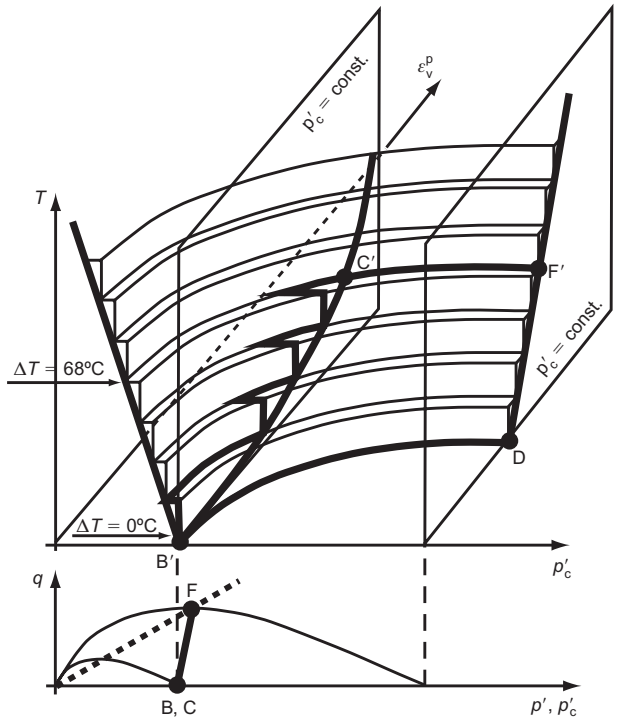

Fig. 9. Representation of a drained heating test at constant stress as conducted on kaolin CH1. Test at 600 kPa, initial OCR = 1 (NC)

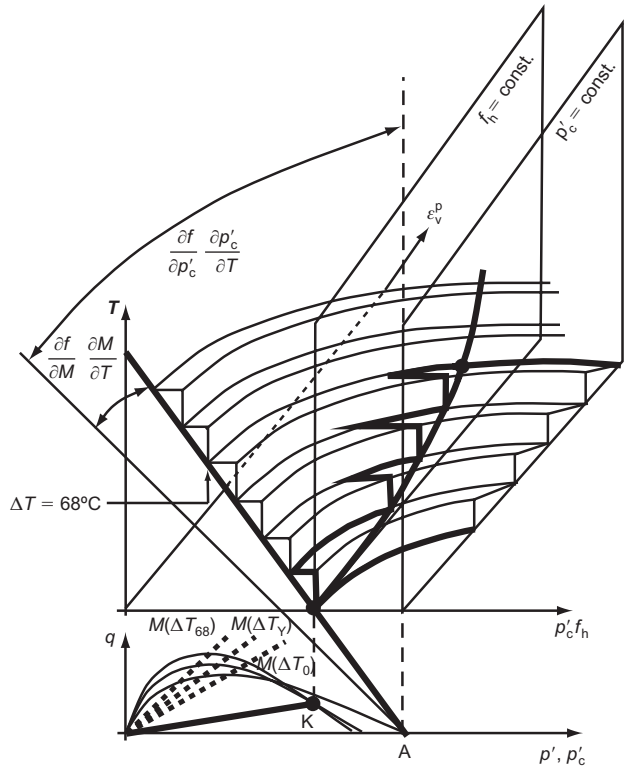

Fig. 10. Schematic of the yield locus evolution and hardening compensatory mechanisms during heating at constant, non-isotropic stress (point *K*) for a temperature-sensitive critical state material, preconsolidated to $p' = p'_{c0} = 600$ kPa

of the integration of the threshold temperatures T_0, T_y and T_f (the initial, isotropic yielding and final temperatures respectively), depending on the constitutive functions $\partial p'_c/\partial T$ and $\partial M/\partial T$.

An analysis of triaxial tests of heated specimens compared with those at room temperature for kaolin CH1, similar to those presented in Fig. 9, may now be performed for the case when $M = M(\Delta T)$. The main difference with respect to the case at M = const. results from the compensation mechanism, which at a generic constant stress state during heating—that is, $q \neq 0$, $\partial M/\partial T \neq 0$—is not controlled by the variable p'_c. In fact, the process is controlled by a less restrictive condition resulting from the compatibility condition of Prager (1958), equation (6), taking the form (Hueckel & Laloui, 2009)

$$\mathrm{d}f_h = \frac{\partial f}{\partial p'_c}\frac{\partial p'_c}{\partial \varepsilon_v^p}\mathrm{d}\varepsilon_v^p + \left(\frac{\partial f}{\partial p'_c}\frac{\partial p'_c}{\partial T} + \frac{\partial f}{\partial M}\frac{\partial M}{\partial T}\right)\mathrm{d}T = 0 \qquad (14)$$

or f_h = const., where

$$f_h = \int \mathrm{d}f\Big|_{\boldsymbol{\sigma}'=\text{const.}} \qquad (15)$$

as shown in the schematic in Fig. 10.

In addition, in contrast to the previous case, the compensating volumetric plastic strain is affected by changes in $M(\Delta T)$, as

$$\mathrm{d}\varepsilon_v^p = \frac{1}{H}\frac{\partial f}{\partial p'}\left(\frac{\partial f}{\partial p'_c}\frac{\partial p'_c}{\partial T} + \frac{\partial f}{\partial M}\frac{\partial M}{\partial T}\right)\mathrm{d}T \qquad (16)$$

Note that the strain rate modes are affected by the above restrictions, which enhance the plastic strain rate vector rotation and the change in plastic volume rate.

To test the effect of the variability of the coefficient of critical state $M(\Delta T)$, numerical simulations of triaxial tests on Kaolin CH1 by Cekerevac & Laloui (2004) were performed, taking into account the linear variability corresponding to the change of $M(\Delta T)$ from $M = 0{\cdot}80$ to $M(90°\mathrm{C}) = 0{\cdot}88$. The results (Fig. 11) confirm the interpretation of stiffer and less compactive stress–strain curves, reflecting the effect of thermal compaction during the heating phase. Predictably, the analysis also shows a higher strength at 90°C than at 22°C, for all paths. This differs from previous simulations performed at a constant M (Laloui & Cekerevac, 2008). The yielding onset in terms of q is lower for 90°C for all overconsolidated stress paths, except at OCR = 1·2 (which is zero), indicating a relatively low sensitivity of the apparent preconsolidation pressure to temperature. Overall, the simulation stress–strain curves at both temperatures are less stiff than the experimental curves. However, this must be attributed to the well-known shortcoming of the original isothermal Cam-clay model.

In conclusion, a number of different patterns of shear strength sensitivity to temperature can be expected from drained clays, depending on whether or not there is a perceptible change (growth in the materials examined) in critical state coefficient, that is, (residual) internal friction angle. If there is no change, or if it is not prominent, the peak stress at high OCR decreases with temperature, but not significantly (20–25%/100°C), whereas normally consolidated and lightly overconsolidated material strength is largely temperature independent. High OCR makes the original dilatant failure more ductile in heated soil, with little volume change.

If there is a thermally induced growth in the critical state coefficient, a very subtle dependence on the heating/loading history develops, with a competition between thermal softening of a decreasing apparent preconsolidation stress and thermal hardening of the internal friction. As a result, the peak stress at high OCR may either decrease or increase with temperature, but not significantly, whereas the strength of normally consolidated and lightly overconsolidated material increases visibly. High OCR can make the original dilatant failure more dilatant,

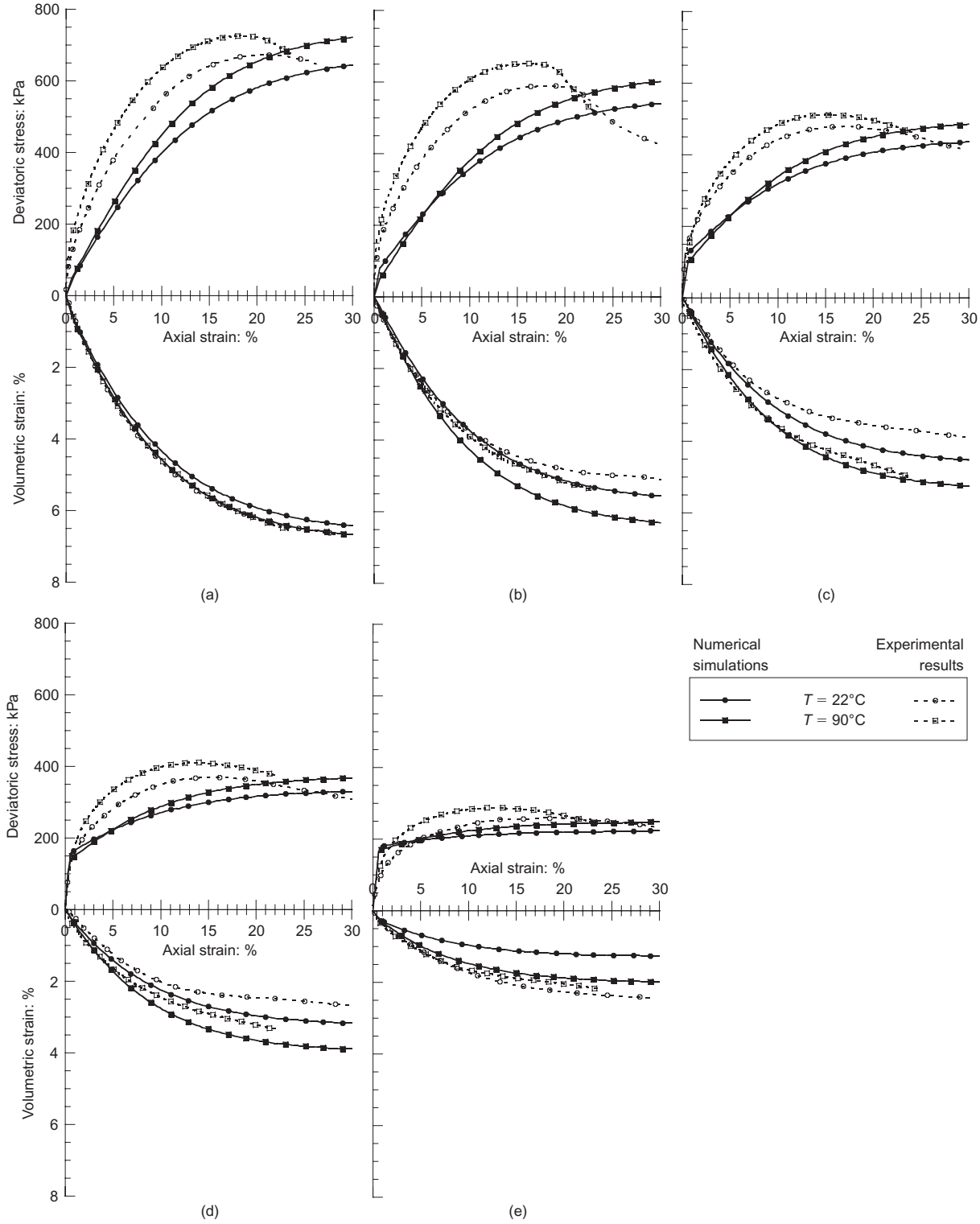

Fig. 11. Results of numerical simulations of triaxial tests on kaolin CH1 (Cekerevac & Laloui, 2004) performed taking into account the linear variability of the coefficient of critical state $M(\Delta T)$, from M = 0·80 to $M(90°C)$ = 0·88: (a) OCR = 1; (b) OCR = 1·2; (c) OCR = 1·5; (d) OCR = 2; (e) OCR = 3

whereas at low OCR the originally compressible shear may become more compactive. The stress at which the heating takes place is critical in the evolution of strength.

Undrained triaxial compression after thermal loading

The central role of the thermomechanical loading history prior to triaxial loading is also found in what is termed 'undrained strength'. Undrained strength is a colloquial expression describing the value of the stress difference at which failure is reached in undrained conditions, depending on the effective stress trajectory and the material history. Hence it is not a material property (see Muir Wood, 1990, 2004). Nevertheless, it is commonly used in geotechnical engineering as such under a set of tacit assumptions. It is briefly examined in three distinct loading modes, in this section and the next.

Consolidated undrained strength. In the first case, heating is performed in drained conditions, and hence at a normally

consolidated state the heating activates the compensatory hardening mechanism, which produces thermoplastic volumetric strain: the higher the temperature, the more consolidated the material at the end of heating. Consequently, in the subsequent undrained triaxial loading, the higher the temperature, the stiffer the triaxial response, and hence this requires less subsequent plastic volumetric strain, similar to what is shown in Fig. 10.

Therefore in undrained compression the temperature effect is manifested through a different form of the effective stress path. Indeed, as during the undrained triaxial compression $\Delta\varepsilon_v = 0$, the process is controlled by the equality of the plastic and elastic volumetric strain increments, $\Delta\varepsilon_v^p = -\Delta\varepsilon_v^e$. The former results from the normality rule, and hence from the slope of the yield locus. The latter strain through elasticity produces a proportional decrease in the mean effective stress, which in turn controls the shape of the effective stress path. Hence, as shown in Fig. 12(b), the higher the temperature, the 'more deviatoric' the effective stress path is, and eventually the higher the maximum deviatoric stress at the failure line, or what is conventionally called the 'undrained strength'.

Experiments of this type were performed by Kuntiwattanakul *et al.* (1995) (Fig. 13), which supported the above prediction. Similar observations were made by Houston *et al.* (1985), Tanaka *et al.* (1997), Burghignoli *et al.* (2000), and Abuel-Naga *et al.* (2006).

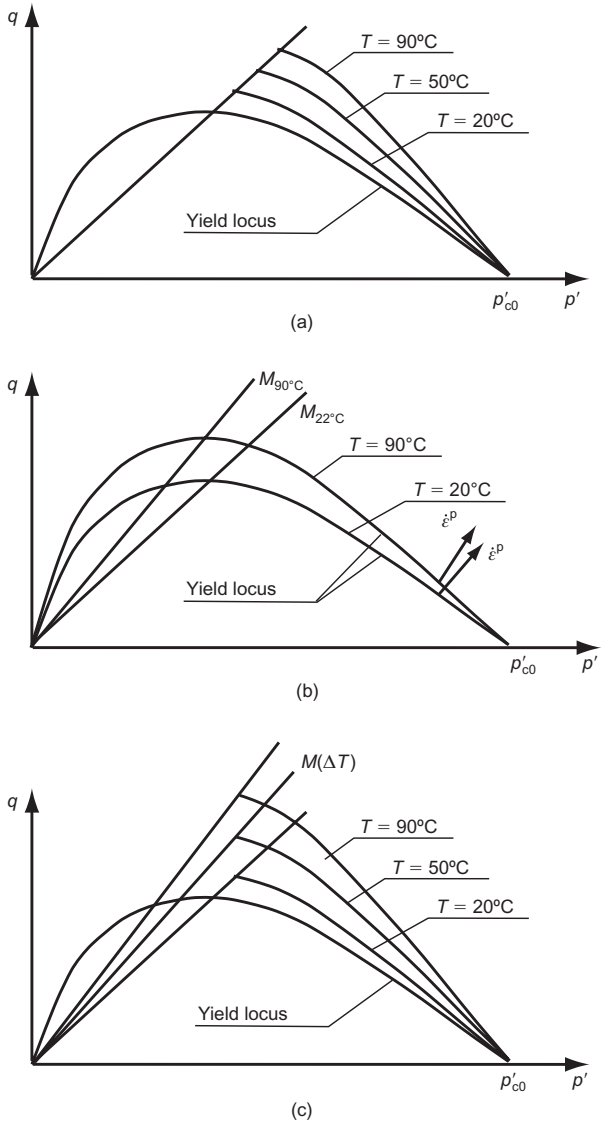

Fig. 12. Schematic of undrained triaxial stress paths for an NC material preceded by drained heating to different temperatures: (a) at M = const.; (b) effect of M on the strain rate mode; (c) at variable M

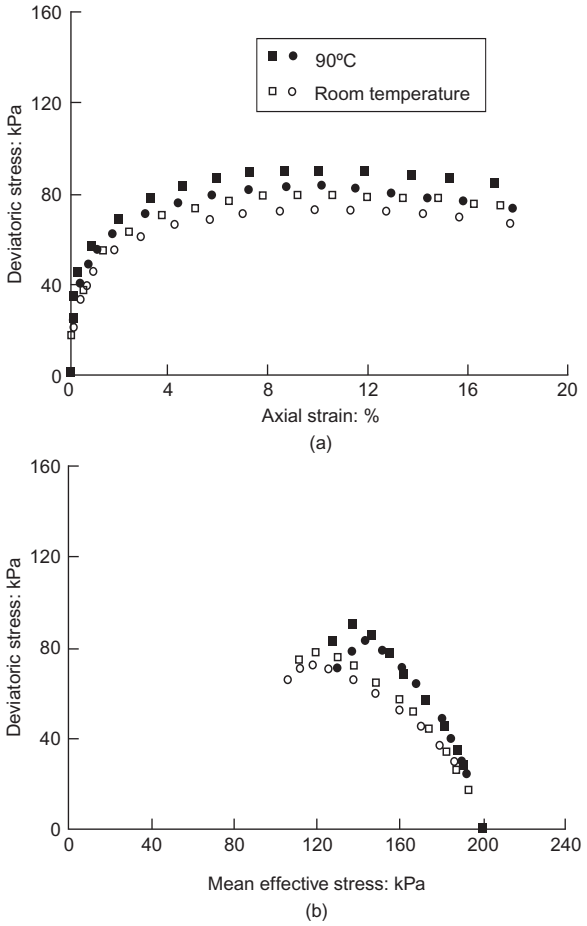

Fig. 13. (a) Stress–strain curves and (b) effective stress paths for triaxial undrained compression tests of drained–heated (and cold) kaolin MC (after Kuntiwattanakul *et al.*, 1995)

The effect of the variable M is twofold: the yield locus normal (i.e. a plastic strain rate vector) has a smaller deviatoric component at higher temperature as the yield locus deviatoric semi-axis grows (Fig. 12(b)). This makes the stress–strain behaviour stiffer. The fact that this also makes the volumetric strain component larger will in part negate the effect on the stress path discussed in the paragraph above. The amount of critical state line rotation with temperature renders the strength slightly higher at higher temperatures (Fig. 12(c)).

The experiments of Houston *et al.* (1985) clearly documented a strong monotonic evolution of M, especially at 200°C. Consequently, the undrained strength increases substantially, also showing an unstable, localised failure. Similarly, Tanaka *et al.* (1997) showed stress–strain curves of undrained tests on a Canadian illite after a drained heating of both NC and OCR = 2 tests, with both indicating a visibly higher undrained strength after heating. No variation in M was reported.

Unconsolidated undrained strength. An alternative way to investigate the sensitivity of undrained strength to temperature is with the so-called 'unconsolidated undrained tests'. Such tests consist of

(*a*) isotropic drained loading to a particular confining stress

in the overconsolidated range, at the normally consolidated state
(*b*) closure of the drainage lines
(*c*) subsequent undrained isotropic heating to a pre-established temperature value, followed by
(*d*) undrained triaxial compression until failure.

Therefore the main difference with respect to the case discussed above is in the fact that, during heating, substantial pore water pressure is generated, hence leading to a reduction in the effective stress. As it increases with the value of the maximum temperature, the subsequent triaxial effective stress paths are clearly far apart and probe differently evolved yield loci.

This kind of test was designed for Boom clay by De Bruyn & Thimus (1996) at different applied confining stresses before the undrained heating. The results qualitatively confirmed the decrease in the size of the yield locus in undrained compression with temperature.

Undrained heating under non-isotropic stress state: thermal failure

This type of test is substantially different from the previous ones, especially in terms of the order of application of the thermal and mechanical loads. The material is first consolidated isotropically and then loaded deviatorically (in undrained or drained conditions) to a stress far below the isothermal undrained failure load. Finally, it is heated in undrained conditions at a constant total stress. A corresponding effective stress path in such experiments for the Boom clay is shown in Fig. 14. The trajectories shown are for different deviatoric stress levels, and include one test (TBoom 2) on a normally consolidated sample (Hueckel *et al.*, 1987; Hueckel & Baldi, 1990) and two tests (TBoom 12 and 14; Hueckel & Pellegrini, 1992; Del Olmo *et al.*, 1996) on overconsolidated (OCR = 3) specimens. In all cases, thermally induced failure through advanced axial strains developed at different temperatures and different pore pressures (Fig. 14(b)), but invariably near the critical state. Several other materials were also tested for this phenomenon (soft Pontida clay, hard Pasquasia clay, and Spanish SS and IC clays), all with similar results. The deviatoric stress undrained heating tests are very important, as they are the best laboratory representation of a worst-case scenario for the stress evolution under field conditions near an embedded heat source, such as in the heating phase of a nuclear waste disposal site (see the boundary value problem simulation in Hueckel *et al.*, 2009).

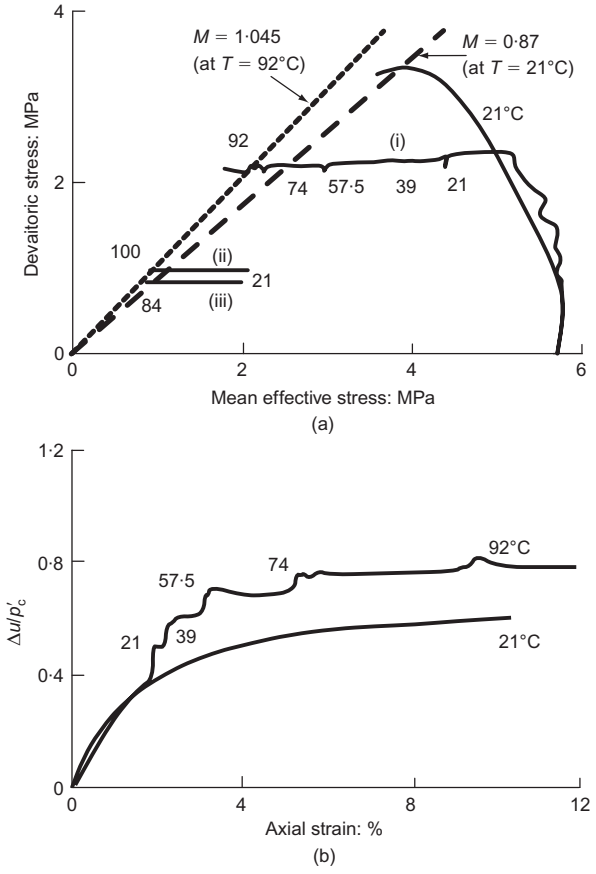

Fig. 14. (a) Effective stress trajectory for constant total stress undrained heating in Boom clay: path (i), test TBoom2; path (ii), test TBoom 12; path (iii), test TBoom 14; (b) pore pressure development during undrained heating at constant deviatoric stress in test TBoom 2 at an initially NC state

The key factor in these tests is the thermally induced pore pressure growth in the presence of a deviatoric stress. The pore water pressure increase is induced by the thermal water volume expansion constrained by five possible factors:

(*a*) the difference between the thermal expansion of pore water and that of the surrounding porous solid under water confinement conditions (undrained heating)
(*b*) mechanical deformation (expansion) of the solids due to isotropic unloading by pore pressure
(*c*) possible thermoplastic compression due to the thermally induced reduction of the yield limit by way of an altered compensation mechanism
(*d*) plastic dilatancy at a lower isotropic stress above the critical line
(*e*) possible thermal release of the adsorbed water into the free pore water, producing an additional pore water volume increase.

As a result of the build-up of pore pressure, the effective stress is reduced from its initial value at the end of the undrained triaxial compression phase at $\Delta T = 0$. At the same time, the yield limit shrinks as a function of temperature. The rates of these two processes are independent from each other, as they are driven by different phenomena. As a result, two alternative scenarios and one 'mixed' scenario are possible.

In Scenario I, the rate of change of the effective stress during the elastic unloading controlled by the thermal increase of pore pressure is higher than the rate of the thermally induced decrease of the yield limit, or in the OC case, the stress point is away from the yield locus. Consequently, effective stress point 1 (Fig. 15) remains detached from the moving yield limit. Hence it remains within the (shrinking) elastic domain. The corresponding strain increment with respect to point C consists of a volumetric expansion, $\Delta\boldsymbol{\varepsilon}^{\mathrm{e}}$, due to a drop in the effective isotropic stress, $\Delta_{\mathrm{c}}\boldsymbol{\sigma}'$, with respect to point C (or pressurisation of water) and thermal expansion of the skeleton, $\Delta\boldsymbol{\varepsilon}^{\mathrm{t}}$. They are represented by normal vectors to, respectively, an elastic potential (in the form of an ellipse $W_{\mathrm{e}}(\Delta_{\mathrm{C}}\sigma') = W_{\mathrm{e}0}$, centred at C) and a thermoelastic potential (a straight line, $W_{\mathrm{t}}(\Delta\sigma', \Delta T)$, as shown in Fig. 15(a),

$$\Delta\boldsymbol{\varepsilon}^{\mathrm{te}} = \frac{\partial W}{\partial \Delta_{\mathrm{C}}\boldsymbol{\sigma}'} = \Delta\boldsymbol{\varepsilon}^{\mathrm{e}} + \Delta\boldsymbol{\varepsilon}^{\mathrm{t}} = \frac{\partial W_{\mathrm{e}}}{\partial \Delta_{\mathrm{C}}\boldsymbol{\sigma}'} + \frac{\partial W_{\mathrm{t}}}{\partial \Delta_{\mathrm{C}}\boldsymbol{\sigma}'} \tag{17}$$

A projection of both strain increment vectors on the σ_1' axis yields the axial strain increment from the onset of heating. As seen in Fig. 15(a), it is a negative—that is, expansive—strain. Such a situation persists until the effective stress point reaches the yield locus at point 2 on the

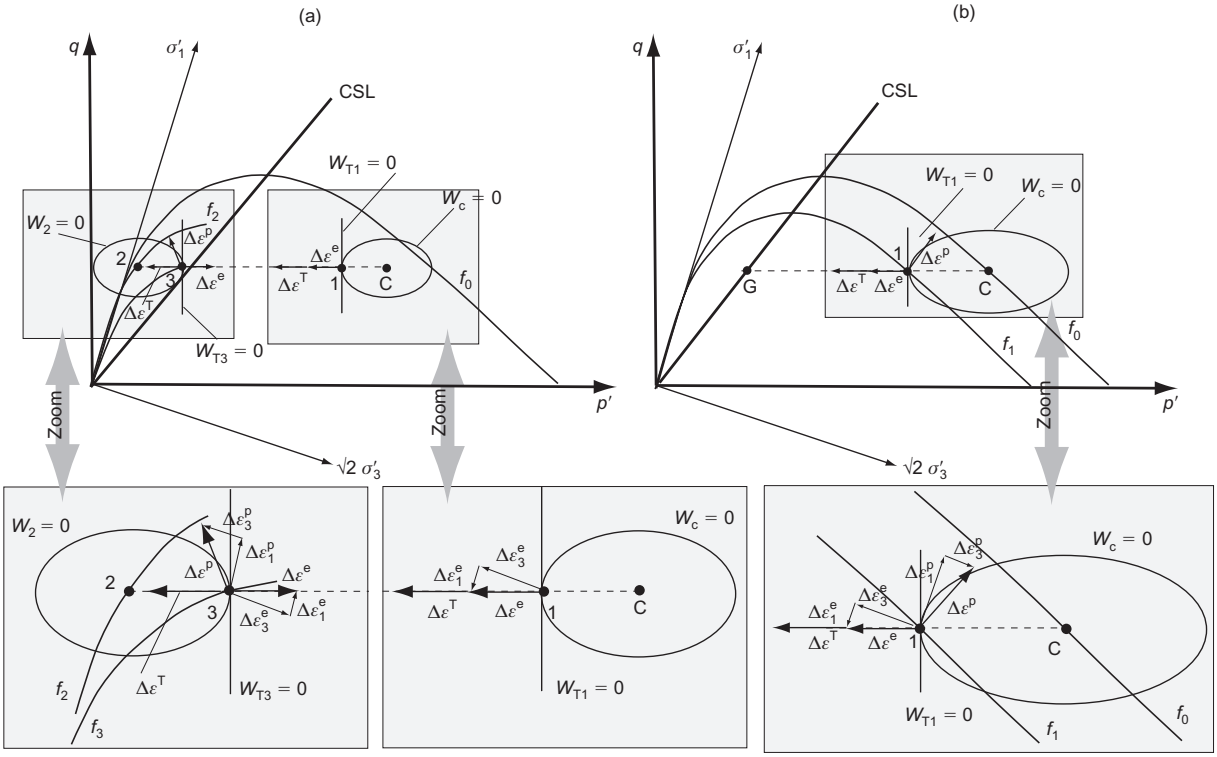

Fig. 15. (a) Scenario I and (b) scenario II, effective stress trajectories and thermo-elasto-plastic strain during undrained constant non-isotropic stress heating for the $M(\Delta T)$ = const. model (after Hueckel & Pellegrini, 1992, and Del Olmo *et al.*, 1996)

strain-softening side. As the process is dominated by the thermal water expansion strain, the only admissible effective stress increment at q = const. at point 2 is towards the interior of the yield locus (e.g. Maier & Hueckel, 1979). The ensuing strain rate increment at a generic point 3 relative to 2 now consists of a similar $\Delta\boldsymbol{\varepsilon}^{t}$ to that at point 1, an opposite $\Delta\boldsymbol{\varepsilon}^{e}$, and an additional thermoplastic strain rate $\Delta\boldsymbol{\varepsilon}^{p}$ normal to the yield locus. The axial components of the two last (and dominant) strain increments are now compressive, as is the axial strain component. The described process ends when it crosses the critical state line, and as for q = const. it becomes inadmissible from the plasticity point of view, implying failure (Maier & Hueckel, 1979). Clearly, there is no 'characteristic temperature at failure', as it depends strongly on the entire history of all the variables involved. The distance between point 2 and the critical line determines the drop in the pore pressure, which occurs despite the continuously increasing temperature. Physically, this is the result of a significant plastic dilatancy starting from point 2, creating pore space to accommodate further water expansion (Fig. 15(a)).

The 'p distance' between the in situ effective stress and the critical state line is likely to be lower in many applications than the pore pressure generated in a given soil with a temperature increase of about 70°C. This is indicative of a potential thermal failure.

In the case where the critical state varies with temperature, $M(\Delta T)$, the above mechanisms remain in place, but the actual 'distances' on the stress trajectory may be significantly altered, both by the higher value of M and by an increased plastic dilatancy. This, in particular, refers to the post-yielding drop in pore pressure, which is expected to decrease with respect to the case of M = const. Hence a variable M is likely to decrease the temperature increase to failure.

In Scenario II, for which the stress point is at or reaches yielding, the rate of change of the effective stress, which is again controlled by the increase of pore pressure, is lower than the rate of the thermally induced decrease of the yield limit. The effective stress point remains constantly at yielding, generating a compressive thermoplastic strain, and thus plastic strain-hardening, which counteracts the thermal softening in a variable sort of compensation mechanism, making the resulting softening rate equal to that of the pore pressure growth.

The corresponding strain rate is dominated by the thermoplastic strain rates, which are visualised by a vector normal to the yield locus, while the thermoelastic strain component is similar to those in Scenario I (Fig. 15(b)). As the axial component of the plastic strain rate is compressive, so is the total axial strain accumulated from the onset of heating. The process may continue until the stress point reaches the critical state at point G. As before, when the yield locus shrinks below the stress level imposed by the condition that q = const., the stress state becomes statically inadmissible. Similarly, there is no 'characteristic temperature to failure', as it depends strongly on the entire history of all the variables involved. The determining factor is rather the pore pressure increase to failure, which is not the case for Scenario I.

Interestingly, in contrast to Scenario I, an increasing $M = M(\Delta T)$ is likely to increase the temperature to failure compared with the M = const. case.

Scenario I was identified in tests TBoom 12 and TBoom 14, starting at OC states, whereas Scenario II was recognised as developing during monotonic heating tests TBoom 2 and TPon 2 on the remoulded Pontida clay (Hueckel & Pellegrini, 1992). The hallmark of Scenario II is a compressive axial strain rate in the presence of an increasing pore pressure. This is distinguished from Scenario I, where a compressive axial strain rate develops from an initial expansive strain at a later stage of heating (at higher temperatures), but is accompanied by a decreasing pore pressure, as seen in TBoom 14. In test TBoom 14, the pore

pressure started decreasing from its maximum value of 1·1 MPa at about 79°C, despite further heating up to 84°C. The drop in pore pressure is not very large (0·11 MPa), but it is persistent.

For further experimental data and discussion of undrained deviatoric thermal failure, including during cyclic heating and cooling, see Hueckel & Pellegrini (1991, 1992) and Del Olmo *et al.* (1996).

An array of 'mixed scenarios' is conceivable, depending on the initial configuration of the yield locus and the initial stress state. In fact, depending on the initial OCR, the initial phase may be elastic, and yielding may occur later on with the effective stress point on the 'hardening side' of the yield locus. Given the non-linearities of both water expansion and hardening functions, all possible combinations of elastic and elasto-plastic state sequences are possible, including a mid-way 'elastic unloading' episode. Note that such possibilities are enhanced at the scale of a boundary value problem (see the companion paper, Hueckel *et al.*, 2009) when a time effect enters the picture. This is due to a time-dependent temperature field coupled with a pore water pressure dissipation as a result of the water outflow from the heated areas driven by the thermally induced high pore pressure gradients.

An overall conclusion from the above analysis is that undrained deviatoric thermal failure is highly dependent on the initial state and history. There is no 'characteristic temperature at failure'; rather, there is a predictable thermal pore pressure increase to failure, but strictly only for Scenario II. For Scenario I, this can be estimated with reasonable accuracy. The value of the pore pressure growth is what makes this process a highly probable occurrence in applications. In other words, it is quite conceivable that the 'p distance' between the in situ effective stress and the critical state line is lower than the pore pressure generated in a given soil with the temperature increase of about 70°C. Clearly, this experiment is only an idealisation of the actual coupled thermo-hydro-mechanical process in situ, as was illustrated in the analysis of the boundary value problem in the companion paper (Hueckel *et al.*, 2009). However, the experiment is at least indicative of the short-term in situ impact.

CONCLUSIONS

This paper presents an attempt to explain apparent contradictions in the results of the dependence of failure criteria on temperature for saturated clays. Conflicting reports of temperature causing strength increases or decreases are cited. Four different failure modes are examined in drained and undrained conditions.

The major conclusion from the above considerations within the framework of Thermal Cam-clay models is that there is no unique a priori answer to the question, at least in the temperature range $4°C < T < 120°C$. First, it appears that the dependence of strength on temperature is material specific. Second, the evolution of both the yield locus and failure is critically dependent on the history of thermomechanical loading, especially the stress state and drainage condition in which the heating is performed. This was suggested earlier by Kuntiwattanakul *et al.* (1995) and Jefferson *et al.* (1996). The compensation mechanism between thermal softening and plastic strain-hardening at constant stress is of critical importance. The mechanism becomes more involved in the presence of variations of the internal friction angle with temperature.

An important issue of the variation (increase) of the critical state coefficient M (or internal friction angle) in some materials with temperature is systematically addressed. It is found that an increase of M not only increases the residual strength in normally consolidated materials, but also may lead to an increase of the peak strength in the overconsolidation range. However, the variation in peak strength is a result of two independent mechanisms: a variation of preconsolidation stress (decrease), and a variation of M (increase). The outcome may be either an increase or a decrease, and also depends on the shape of the yield locus. The deformation mode of heated specimens in triaxial tests is equally strongly dependent on the entire thermoplastic history. Some previous, seemingly unusual, findings now appear to be logically explained by the observed concomitant increase of the critical state coefficient.

It is concluded that there is no single yield surface that can be attributed uniquely to a given temperature. Indeed, the yield limit generated during the same heating phase in each of the cases depends on the level of confining stress and OCR, and the response during thermoplastic heating.

A schematic boundary value problem of the coupled thermo-hydro-mechanical response of a clay mass to a cylindrical heat source is examined in the companion paper (Hueckel *et al.*, 2009). It shows that the variation of the effective internal friction angle with temperature may have a substantial influence on the margin of safety.

A natural question hence arises: what makes the internal friction of some materials sensitive to temperature increase, while others are not at all sensitive to temperature increase? There is no direct experimental evidence available at present to answer this question. However, studies in the area of soil contamination have indicated differences in the response of water adsorbed on clay to physico-chemical changes in different minerals. The role of adsorbed water in controlling compressibility and internal friction in clays may provide a clue to their peculiar sensitivity to heat (Sridharan & Venkatappa Rao, 1973). The removal or decrease in thickness of the adsorbed water from the particle edge area (particle contact) has been suggested to increase their friction (and hence the coefficient M). This is more likely to occur in kaolin, which has only external adsorbed water. As smectites house their adsorbed water between the platelets within the cluster particles, its removal affects mainly the compressibility (and hence the apparent preconsolidation parameter p'_c) and much less the internal friction (Mitchell & Soga, 2005). Experimental and molecular dynamics simulation studies of clay adsorbed water have pointed out that elevated temperature disrupts the adsorbed water, and that the thickness of the adsorbed layer strongly affects the viscosity of interparticle contacts. Such properties were found to occur at a much higher rate than previously thought (Claesson *et al.*, 1986; Cushman, 1990; Huang *et al.*, 1994). Hence it is speculated that the adsorbed water plays a different structural role in the differentiated response of clay minerals to heating.

This study points out some novel correlations between various aspects of the thermomechanical behaviour of clays. It also reveals that comprehensive experimental and modelling studies are needed to provide a confident assessment of the response of geotechnical structures subjected to elevated temperatures.

NOTATION

$d\lambda$	plastic multiplier
e	void ratio
e_0	initial void ratio
f	yield limit
H	hardening modulus
M	slope of critical state line in the p′-q plane
OCR	overconsolidation ratio
p'	mean effective stress

p'_c	apparent preconsolidation stress
p'_{c0}	initial apparent preconsolidation pressure
q	deviatoric stress
$\tilde{q}$	peak strength
$q*$	minor semi axis of the yield locus
q_{crit}	residual strength
T	temperature in °C
T_0	initial temperature
T_f	final temperature
T_y	temperature at yielding
W_e	elastic potential
W_t	thermoelastic potential
ΔT	temperature variation
ε_v^e	volumetric elastic strain
ε_v^p	volumetric plastic strain
ε_1	axial strain
ε_v	volumetric strain
γ, a_0, a_1, a_2	material parameters for evolution of preconsolidation pressure with temperature
κ	isotropic moduli of elastic incremental compressibilities of soil
λ	isotropic moduli of elasto-plastic incremental compressibilities of soil
$\boldsymbol{\sigma}'$	effective stress

REFERENCES

Abuel-Naga, H. M., Bergado, D. T., Ramana, G. V., Grino, L., Rujivipat, P. & Thet, Y. (2006). Experimental evaluation of engineering behavior of soft Bangkok clay under elevated temperature. *J. Geotech. Geoenviron. Engng* **132**, No. 7, 902–910.

Argon, A. S. (2001). Mechanics and physics of brittle to ductile transitions in fracture. *J. Engng Mater. Technol. ASME* **123**, No. 1, 1–11.

Baldi, G., Hueckel, T. & Pellegrini, R. (1988). Thermal volume change of the mineral–water system in low-porosity clay soils. *Can. Geotech. J.* **25**, No. 4, 807–825.

Baldi, G., Hueckel, T., Peano, A. & Pellegrini, R. (1991). *Developments in modelling of thermo-hydro-mechanical behaviour of Boom clay and clay-based buffer materials, Vols 1 and 2*, EUR 13365/1 and 13365/2. Luxembourg: Commission of the European Communities.

Baldi, G., Borsetto, M. & Pellegrini, R. (1993). Medium scale laboratory tests for the interpretation of predictive models of the thermomechanical properties of clay barriers. *Proceedings of the international workshop on thermo-mechanics of clays and clay barriers*, Seriate (Bergamo), Section 3, 43–63.

Bigoni, D. & Hueckel, T. (1991). Uniqueness and localization – I. Associative and non-associative elastoplasticity. *Int. J. Solids Struct.* **28**, No. 2, 197–213.

Borsetto, M., Cricchi, D., Hueckel, T. & Peano, A. (1984). On numerical models for the analysis of nuclear waste disposal in geological clay formations In *Numerical methods for transient and coupled problems* (ed. R. W. Lewis), pp. 608–618. Swansea: Pineridge Press.

Bourros, C. M. (1973). *The effect of temperature change on consolidation and shear strength of saturated cohesive soils*. PhD dissertation, University of Washington.

Brandl, H. (2006). Energy foundations and other thermo-active ground structures. *Géotechnique* **56**, No. 2, 81–122.

Burghignoli, A., Desideri, A. & Miliziano, S. (2000). A laboratory study on the thermomechanical behaviour of clayey soils. *Can. Geotech. J.* **37**, No. 4, 764–780.

Campanella, R. G. & Mitchell, J. K. (1968). Influence of temperature variations on soil behavior. *J. Soil Mech. Found. Div. ASCE* **94**, No. 3, 709–734.

Cekerevac, C. & Laloui, L. (2004). Experimental study of thermal effects on the mechanical behaviour of a clay. *Int. J. Numer. Anal. Methods Geomech.* **28**, No. 3, 209–228.

Claesson, P. M., Kjellander, R., Stenius, P. & Christenson, H. K. (1986). Direct measurement of temperature-dependent interactions between non-ionic surfactant layers. *J. Chem. Soc. Faraday Trans. I* **82**, No. 9, 2735–2746.

Cui, Y. J., Sultan, N. & Delage, P. (2000). A thermomechanical model for saturated clays. *Can. Geotech. J.* **37**, No. 3, 607–620.

Cushman, J. (1990). Molecular scale lubrification. *Nature* **347**, 227–228.

De Bruyn, D. & Thimus, J. F. (1996). The influence of temperature on mechanical characteristics of Boom clay: the results of an initial laboratory programme. *Engng Geol.* **41**, Nos. 1–4, 117–126.

Del Olmo, C., Fioravante, V., Gera, F., Hueckel, T., Mayor, J. C. & Pellegrini, R. (1996). Thermomechanical properties of deep argillaceous formations. *Engng Geol.* **41**, Nos. 1–4, 87–102.

Drescher, A., Hueckel, T. & Mróz, Z. (1974). Multiple shear method for anisotropic chemical powders. *Bull. Industrial Chemistry* **4**, No. 22, 3–18.

François, B. & Laloui, L. (2008). ACMEG-TS: a constitutive model for unsaturated soils under non-isothermal conditions. *Int. J. Numer. Anal. Methods Geomech.* **32**, No. 16, 1955–1988.

Gens, A. & Olivella, S. (2001). Clay barrier in radioactive waste disposal. *Rev. Fr. Génie Civil* **5**, No. 6, 845–856.

Gera, F., Hueckel, T. & Peano, A. (1996). Critical issues in modelling of the long-term hydro-thermal performance of natural clay barriers. *Engng Geol.* **41**, Nos 1–4, 17–33.

Hahn, D. E., Burke, L. H., Mackenzie, S. F. & Archibald, K. H. (2003). Completion design and implementation in challenging HP/HT wells in California. *SPE: Drilling & Completion* **18**, No. 4, 293–303.

Houston, S. L., Houston, W. N. & Williams, N. D. (1985). Thermomechanical behavior of seafloor sediments. *J. Soil Mech. Found. Div. ASCE* **111**, No. 11, 1249–1263.

Huang, W. L., Basset. W. A. & Wu, T. C. (1994). Dehydration and rehydration of montmorillonite at elevated pressures and temperatures monitored using synchrotron radiation. *Am. Mineral.*, **79**, Nos 7–8, 683–691.

Hueckel, T. (1992). Water–mineral interaction in hygromechanics of clays exposed to environmental loads: a mixture-theory approach. *Can. Geotech. J.* **29**, No. 6, 1071–1086.

Hueckel, T. (1997). Chemo-plasticity of clays subjected to stress and flow of a single contaminant. *Int. J. Numer. Anal. Methods Geomech.* **21**, No. 1, 43–72.

Hueckel, T. & Baldi, G. (1990). Thermoplasticity of saturated clays: experimental constitutive study. *J. Geotech. Engng* **116**, No. 12, 1778–1796.

Hueckel, T. & Borsetto, M. (1990). Thermo-plasticity of saturated soils and shales: constitutive equations. *J. Geotech. Engng* **116**, No. 12, 1765–1777.

Hueckel, T. & Laloui, L. (2009). Implications of thermal sensitivity of the internal friction angle. *Proc. 1st Int. Symp. Comp. Geomech. (ComGeo1), Juan-les-Pins*, France.

Hueckel, T. & Pellegrini, R. (1989). Modeling of thermal failure of saturated clays. *Proc. 3rd Int. Symp. on Numerical Models in Geomechanics, Niagara Falls*, 81–90.

Hueckel, T. & Pellegrini, R. (1991). Thermoplastic modeling of undrained failure of saturated clay due to heating. *Soils Found.* **31**, No. 3, 1–16.

Hueckel, T. & Pellegrini, R. (1992). Effective stress and water pressure in saturated clays during heating-cooling cycles. *Can. Geotech. J.* **29**, No. 6, 1095–1102.

Hueckel, T., Borsetto, M. & Peano, A. (1987). Modelling of coupled thermo-elasto-plastic- hydraulic response of clays subjected to nuclear waste heat. In *Numerical methods in transient and coupled problems* (eds R. W. Lewis *et al.*), pp. 213–235. Chichester: John Wiley.

Hueckel, T., Peano, A. & Pellegrini, R. (1993). A constitutive law for thermo-plastic behaviour of rocks: an analogy with clays. *Surveys Geophys.* **15**, No. 5, 643–671.

Hueckel, T., Pellegrini, R. & Del Olmo, C. (1998). A constitutive study of thermo-elasto-plasticity of deep carbonatic clays. *Int. J. Numer. Anal. Methods Geomech.* **22**, No. 7, 549–574.

Hueckel, T., Francois, B. & Laloui, L. (2009). Temperature dependent internal friction angle in heating source experiments in clay mass. *Géotechnique* (under review).

Jefferson, I., Rogers, C. D. F. & Smalley, I. J. (1996). Discussion: 'Temperature effects on undrained shear characteristics of clay' by Kuntiwattanakul *et al.* (1995). *Soils Found.* **36**, No. 3, 141–143.

Kovari, K. & Tisa, A. (1975). Multiple failure state and strain controlled triaxial tests. *Rock Mech.* **7**, No. 1, 17–33.

Kuntiwattanakul, P., Towhata, I., Ohishi, K. & Seko, I. (1995).

Temperature effects on undrained shear characteristics of clay. *Soils Found.* **35**, No. 1, 147–162.
Laloui, L. (1993). *Modélisation du comportement thermo-hydro-mécanique des milieux poreux anélastique*. PhD thesis, Ecole Centrale, Paris.
Laloui, L. & Cekerevac, C. (2003). Thermo-plasticity of clays: an isotropic yield mechanism. *Comput. Geotech.* **30**, No. 8, 649–660.
Laloui, L. & Cekerevac, C. (2008). Numerical simulation of the non-isothermal mechanical behaviour of soils. *Comput. Geotech.* **35**, No. 5, 729–745.
Laloui, L., Nuth, M. & Vulliet, L. (2006). Experimental and numerical investigations of the behaviour of a heat exchanged pile. *Int. J. Numer. Anal. Methods Geomech.* **30**, No. 8, 763–781.
Laloui, L., François, B., Nuth, M., Peron, H. & Koliji, A. (2008). A thermo-hydro-mechanical stress–strain framework for modelling the performance of clay barriers in deep geological repositories for radioactive waste. *Proc. 1st Eur. Conf. on Unsaturated Soils, Durham*, 63–80.
Maier, G. & Hueckel, T. (1979). Nonassociated and coupled flow-rules of elastoplasticity for rock-like materials. *Int. J. Rock Mech. Min. Sci.* **16**, No. 2, 77–92.
Marques, M. E. S., Leroueil, S. & Almeida, M. S. S. (2004). Viscous behaviour of the St-Roch-de l'Achigan clay, Quebec. *Can. Geotech. J.* **41**, No. 1, 25–38.
Mitchell, J. K. (1964). Shearing resistance of soils as a rate process. *J. Soil Mech. Found. Engng Div. ASCE* **90**, No. 1, 231–251.
Mitchell, J. K. & Soga, K. (2005). *Fundamentals of soil behavior*, 3rd edn. Chichester: John Wiley.
Muir Wood, D. (1990). *Soil behaviour and critical state soil mechanics.* Cambridge: Cambridge University Press.
Muir Wood, D. (2004). *Geotechnical modelling*. Abingdon: Spon Press.
Picard, J. M. (1994). *Ecrouissage thermique des argiles saturées: application au stockage de déchets radioactifs*. PhD thesis, Ecole Nationale des Ponts et Chaussées, Paris.
Plum, L. & Esrig, M. I. (1969). *Some temperature effects on soil compressibility and pore water pressure: Special report*, Report 103. Washington: Highway Research Board.
Prager, W. (1958). Non-isothermal plastic deformation. *Koninkklijk-Nederland Akademie Van Wetenschappen Te Amsterdam*, **61**, No. 3, 176–182.
Roscoe, K. H. & Burland, J. B. (1968). On the generalised stress–strain behavior of wet clay. In *Engineering plasticity* (eds J. Heyman and F. A. Leckie), pp. 535–609. Cambridge: Cambridge University Press.
Rousset, G. (1992). *Etude experimentale du comportement de l'argile de l'Aisne, Partie 1 & 2*, internal reports G3S (LMS, Ecole Polytecnique, Palaiseau) 92-002 and 92-005. Palaiseau: G3S.
Schofield, A. & Wroth, P. (1968). *Critical state soil mechanics*. London: McGraw-Hill.
Sridharan, A. & Venkatappa Rao, G. (1973). Mechanisms controlling volume change of saturated clays and the role of the effective stress concept. *Géotechnique* **23**, No. 3, 359–382.
Tanaka, N., Graham, J. & Crilly, T. (1997). Stress–strain behaviour of reconstituted illitic clay at different temperatures. *Engng Geol.* **47**, No. 4, 339–350.
Wong, T.-F. (1982). Effects of temperature and pressure on failure and post-failure behavior of Westerly Granite. *Mech. Mater.* **1**, No. 1, 3–17.